OPEN ACCESS Freely available online

AFM Applied Functional Materials

ISSN 2737-5323
Volume 2, Issue 2
https://www.iikii.com.sg/journal/AFM
Applied Functional Materials

Article

Pressure and Thickness Dependence of Physical Properties of ZnO:Ga Thin Films by Radio Frequency Magnetron Sputtering

Fang-Hsing Wang [1,2,*] and Hua-Tz Tzeng [2]

[1] Department of Electrical Engineering, National Chung-Hsing University, Taichung 402, Taiwan, R.O.C.;
[2] Graduate Institute of Optoelectronic Engineering, National Chung-Hsing University, Taichung 402, Taiwan, R.O.C.;
edison76513@yahoo.com.tw
* Correspondence: fansen@dragon.nchu.edu.tw; Tel.:+886-4-22840688 ext. 706

Received: May 23, 2022; **Accepted:** Jun 23, 2022; **Published:** Jun 30, 2022

Abstract: Indium-free transparent conducting oxide films have attracted extensive attention in the field of optoelectronics. Ga-doped ZnO (GZO) thin films are deposited by radio frequency magnetron sputtering on glass substrates at a temperature of 200 °C with ZnO:Ga_2O_3 (3 wt%). The structural, electrical, and optical properties of the GZO thin films were investigated in terms of deposition pressure and film thickness variations. X-ray diffraction analysis showed that all the prepared GZO films exhibited hexagonal wurtzite crystal structure with a (002) preferential orientation along the c-axis, regardless of pressure and thickness. The average visible transmittance (including the glass substrate) in a wavelength range of 400–700 nm decreased with increasing thickness but varied less with pressure. The highest average visible transmittance reached 88.4% at the thickness of 150 nm and the pressure of 5 mTorr. The optical band gap of the GZO films calculated using Tauc's method was in the range of about 3.6–3.9 eV. The resistivity of GZO thin films decreased with decreasing deposition pressure and increasing film thickness, and the minimum resistivity obtained at 5 mTorr and 1000 nm was 3.36×10^{-4} Ω-cm. The maximum figure of merit (*FOM*) of 3.09×10^{-2} Ω^{-1} was achieved at 5 mTorr and 1000 nm. The superior optical and electrical properties and high *FOM* show that the prepared GZO thin films are suitable for transparent conducting films and optoelectronic devices.

Keywords: Ga-doped ZnO (GZO), Pressure, Thickness, Transparent conducting oxide (TCO), Magnetron sputtering

1. Introduction

Transparent conducting oxide (TCO) thin films are widely used in numerous optoelectronic devices, such as flat-panel displays, photovoltaic cells, and smart windows. The tin-doped indium oxide (In_2O_3:Sn, ITO) thin film has the advantages of low resistivity (~10^{-4} Ω-cm) and high transmittance (>85%) and is the most commonly used TCO material in the past two decades [1,2]. However, indium is a moderately toxic metal and is relatively rare (0.049 ppm) in the Earth's crust. In addition, amorphous ITO films are not stable in a high temperature (>250 °C) environment. Therefore, researchers are constantly looking for alternative materials for ITO thin films.

Because of abundance in nature, easy fabrication at low temperature, non-toxicity, large direct band gap energy (3.37 eV), and good chemical/thermal stability, doped zinc oxide (ZnO) thin film is expected to be substituted for ITO as a promising TCO film. Among various possible dopants, ZnO thin films doped with the group-13 elements, such as ZnO:Al [3–5], ZnO:Ga [6–12], and ZnO:In [13] exhibited high electrical conductivity and transparency in the visible spectral range and have been extensively studied over the past two decades. Minami et al. reviewed TCO thin films and reported that the ZnO:Al and ZnO:Ga thin films with a resistivity of the order of 1×10^{-4} Ω-cm were prepared by using pulsed laser deposition and vacuum arc plasma evaporation [6]. We also used the ZnO:Ga thin film as a front transparent electrode to fabricate amorphous silicon thin film solar cells [9].

In the current study, Ga-doped ZnO (GZO) thin films with a 3 wt% dopant were prepared on glass substrates by using radio frequency (RF) magnetron sputtering. Influences of deposition pressure and film thickness on optical, electrical, and structural properties of sputtered GZO films were explored and discussed.

2. Materials and Methods

The Corning EagleXG glass substrates were cleaned sequentially in deionized water, acetone, and isopropanol in an ultrasonic bath in each step for 10 min. After cleaning and drying these substrates, GZO thin films were physically deposited on the glass substrates using an RF magnetron sputtering system (Syskey Co., SKE-95015). The sputtering target with a diameter of 2 in and a

thickness of 5 mm was prepared with zinc oxide powders mixed with 3 wt% gallium oxide powders. The working distance was fixed at 8 cm. The base pressure was pumped to 6.67×10^{-4} Pa (5×10^{-6} Torr) by a turbomolecular pump and a dry pump. The working pressure varied from 0.667 to 6.67 Pa (5 to 50 mTorr). During sputtering, the RF power was fixed at 50 W and the substrate temperature was maintained at 200 °C. The thickness of GZO thin films ranged from 70 to 1500 nm.

A spectroscopic ellipsometer (Nano-view SE MF-100) was used to measure the thickness of the prepared GZO film. X-ray diffraction (XRD, PANalytical) analysis with Cu-Kα radiation (λ = 1.54056Å) was carried out to investigate crystal orientation and quality. The resistivity, carrier concentration, and Hall mobility of the film were measured by the four-point probe method (Napson RT-70) and the Hall-effect measurement method (ECOPIA, HMS-3300). An ultraviolet-visible spectrophotometer (Hitachi U-3300) was used to determine the optical transmittance of the film in the wavelength range of 300–800 nm. All measurements were made at room temperature (20 to 25 °C) and ambient pressure.

3. Results

Figure 1 shows the deposition rate of the GZO thin films as a function of deposition pressure and film thickness. From Fig. 1(a), it was found that the deposition rate strongly depended on deposition pressure. As the pressure increased from 5 to 50 mTorr, the deposition rate significantly decreased from 6.7 to 3.2 nm/min. In general, the mean free path of sputtered particles is inversely proportional to the sputtering pressure. Thus, this result can be explained by the higher deposition pressure that results in a shorter mean free path and more collisions of sputtered particles as these particles travel from the target to substrates. Therefore, more sputtered particles were scattered and the deposition rate decreased. Zhou et al. also found a similar trend in that the deposition rate of Al-doped ZnO films increased with decreasing sputtering pressure [14]. On the other hand, the dependence of deposition rate on film thickness was not significant. When we changed the thickness of the GZO thin films from 70 to 1500 nm, the deposition rate almost remained at about 6.7 nm/min, as Fig. 1(b) shows. This result suggests that the deposition rate is almost constant for different sputtering times.

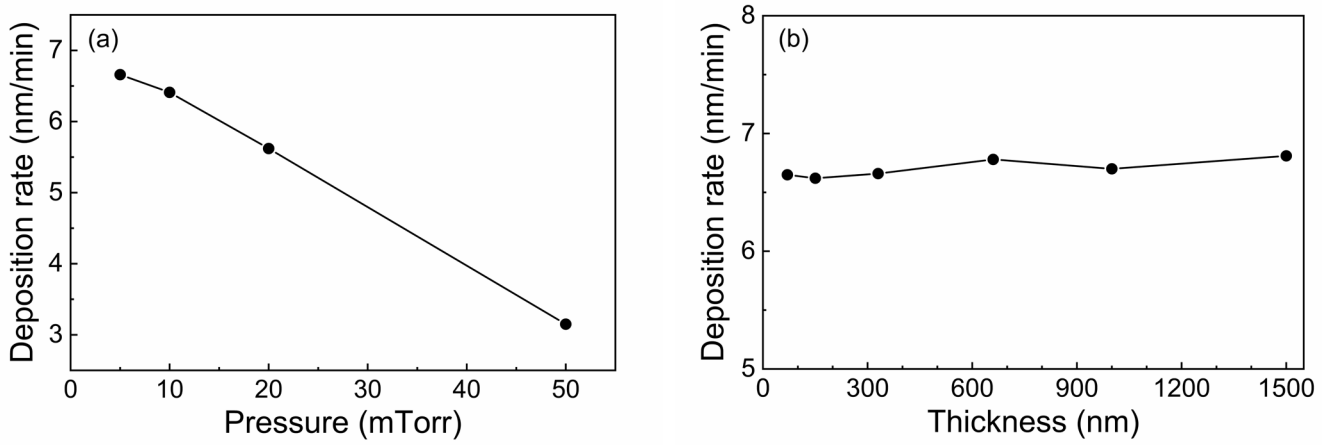

Fig. 1. Deposition rate of the GZO thin films as a function of (a) deposition pressure and (b) film thickness.

Figure 2 shows XRD patterns of the GZO thin films deposited with different deposition pressures and film thicknesses. All GZO films exhibited the (0 0 2) peak at around 2θ ~ 34°, which reveals that the GZO thin films deposited by RF magnetron sputtering have a polycrystalline crystal with the hexagonal wurtzite structure and are preferentially oriented along the c-axis perpendicular to the substrate. The c-axis crystal orientation of the GZO thin films is understood with the "survival of the fastest" model proposed by Drift [15]. Additionally, no Ga_2O_3 phase was found from the XRD patterns for all samples, suggesting that gallium may substitute zinc in the ZnO lattice site to form a Ga-O bond or segregate into the grain boundary region. It is worth noting that the intensity of the (0 0 2) peak decreased with increasing pressure while it increased with increasing film thickness. This result shows that the crystal quality of the sputtered GZO films is closely related to the deposition pressure and film thickness. GZO films have better crystallinity at lower deposition pressures (5 mTorr) and larger film thicknesses (1500 nm). In addition, the (0 0 2) peak position slightly shifted to the high angle side with decreasing deposition pressure or increasing film thickness. It is because the ionic radius of Ga is smaller than that of Zn and Ga atoms are ionized into Ga^{3+} and substitute Zn^{2+} in the lattice site. Thus, the lattice parameter c of films becomes shorter [16]. Meng and Santos [17] also investigated the effect of total pressure on the (0 0 2) peak height of RF magnetron sputter-grown ZnO thin films. Their XRD results showed that the (0 0 2) peak intensity increased as the total pressure increased from 0.2 Pa

(1.5 mTorr) to 0.6 Pa (4.5 mTorr) and then decreased as the pressure increased further to 3 Pa (22.5 mTorr). Their result is similar to that of the GZO thin films prepared at 5–50 mTorr in this work.

Figure 3 presents the full width at half-maximum (FWHM) and grain size of GZO thin films as a function of deposition pressure and film thickness. Scherrer's formula is used to estimate the average grain size in the vertical direction of the crystal [18],

$$D = \frac{0.94\lambda}{\beta \cos\theta} \quad (1)$$

where D is the diameter of the grain, β is the FWHM, and λ is the wavelength of the Cu-Kα line (λ = 1.54 Å. Figure 3(a) shows that as the deposition pressure increased from 5 to 50 mTorr, the FWHM increased from 0.2° to around 0.3°, and meanwhile the grain size decreased from 41 to around 28 nm. The reduced grain size is attributed to the weak particle bombardment and low surface diffusion energy of the films deposited at high sputtering pressures. When the film thickness increased from 70 to 1500 nm, the FWHM decreased from 0.35° to 0.22°, while the grain size increased from 24 to 38 nm, as shown in Fig. 3(b). This result shows that the crystal quality of the GZO film was enhanced as its thickness increased. This phenomenon is similar to Ga (2%) doped ZnO films as reported by Wu et al. [19].

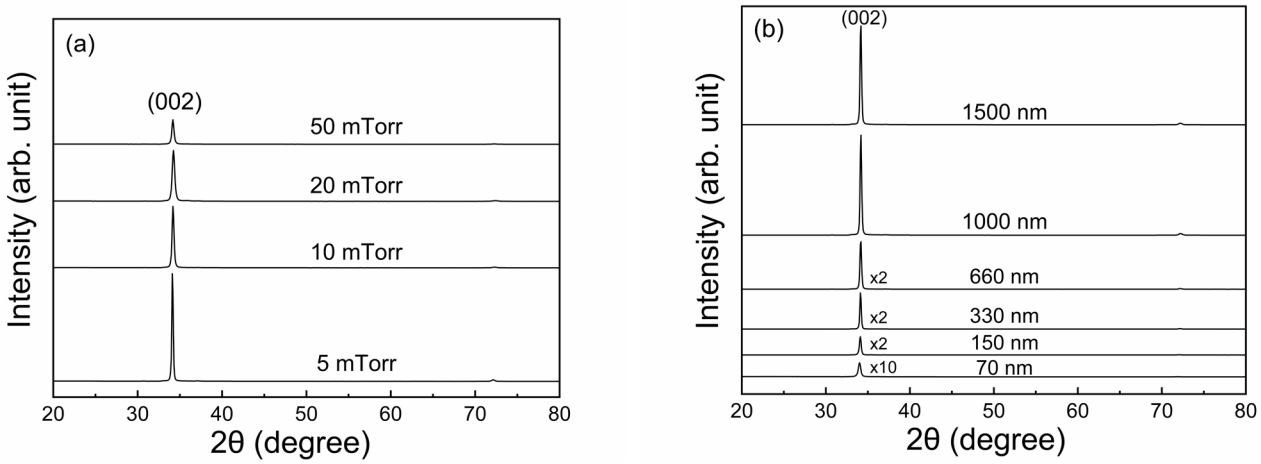

Fig. 2. XRD patterns of the GZO thin films with various (a) deposition pressures and (b) film thickness.

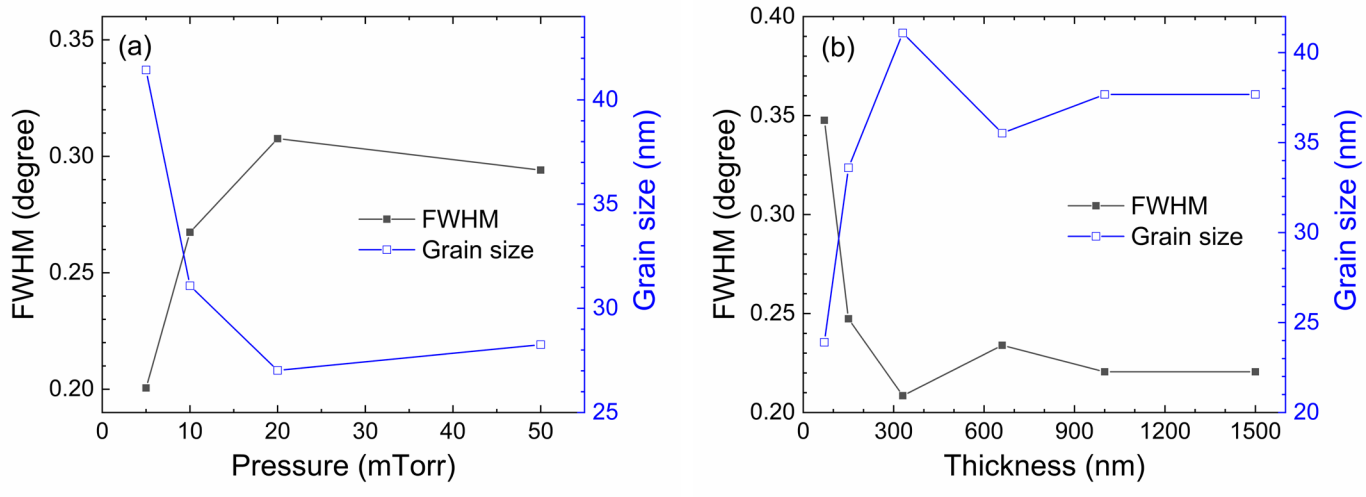

Fig. 3. Full-width at half-maximum (FWHM) and grain size of the GZO thin films as a function of (a) deposition pressures and (b) film thickness.

The electrical properties of the GZO films were characterized by the Hall effect measurement. Figure 4 shows the resistivity, Hall mobility, and carrier concentration of the GZO thin films with various deposition pressures and film thicknesses. Figure 4(a) presents that both the carrier concentration (n) and Hall mobility (μ) decreased with the increasing pressure. According to $\rho = 1/(qn\mu)$, where q is the electron charge and ρ is resistivity, the resistivity increased from 5.25×10^{-4} to 4.12×10^{-3} Ω-cm as the pressure increased from 5 to 50 mTorr. In Fig. 4(b), it is observed that as the film thickness increases from 70 to 1500 nm, the Hall mobility increased from 11.7 to 18.6 cm^2/V-sec, and the carrier concentration also increases from 6.63×10^{20} cm^{-3} to a maximum of 1.06×10^{21} cm^{-3} at a thickness of 1000 nm, while the resistivity decreased form 8.05×10^{-4} to a minimum of 3.36×10^{-4} Ω-cm. Resistivity is inversely proportional to the product of carrier concentration and Hall mobility. The increase of resistivity in the high pressure and thin thickness region is associated with decreases in both the electron density and electron mobility. The low resistivity in the low deposition pressure and thick film thickness region is due to the improved crystallinity and more extrinsic/intrinsic donors in the GZO films. As shown by the XRD data, the superior crystal quality of the GZO films prepared with low pressure and high film thickness afforded better electrical characteristics [20]. Similar electrical behavior as a function of thickness was reported by Wu et al. and Shin et al. [19,20]. Wu et al. reported that the lowest resistivity of 3.685×10^{-3} Ω-cm occurred in their thickest GZO film (t = 620 nm) [20]. Our earlier study also showed that the resistivity of the ZnO:Ti thin film decreased from 3.94×10^{-2} to 1.06×10^{-3} Ω-cm when the film thickness increased from 30 to 950 nm [21].

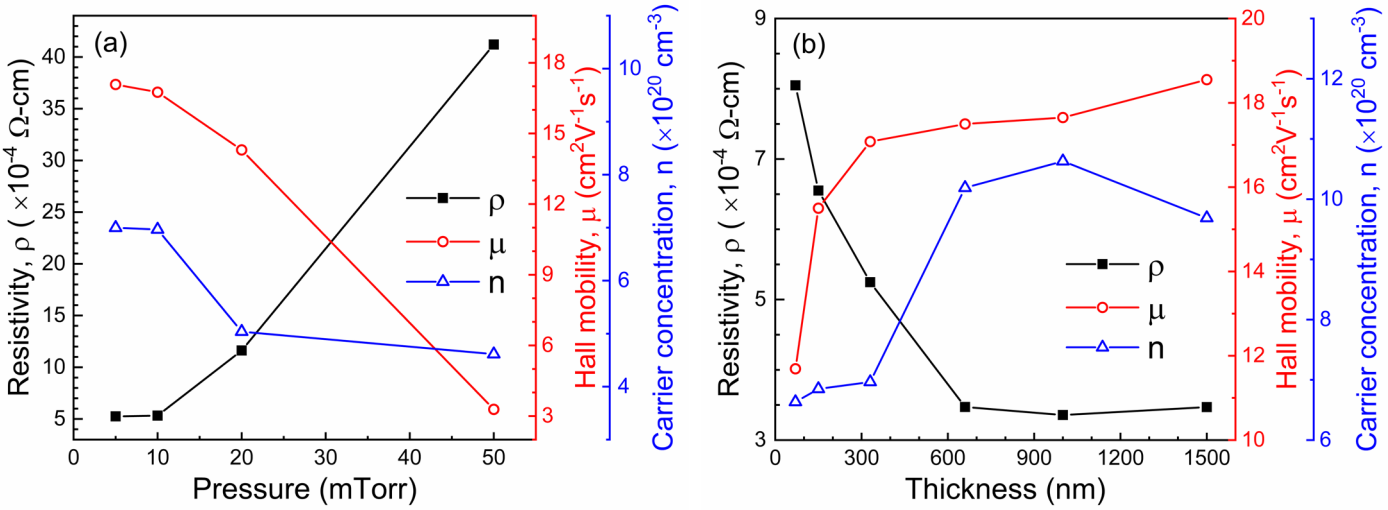

Fig. 4. Resistivity, Hall mobility, and carrier concentration of the GZO thin films as a function of (a) deposition pressure and (b) film thickness.

Figure 5 exhibits the optical transmission spectra of the GZO thin films in the wavelength region of 300–800 nm with different deposition pressures and film thicknesses. Figure 5(a) shows that the average optical transmission of the GZO film (including the glass substrate) in the visible wavelength range (400–700 nm) was in the range of 84%–86%. Notably, the deposition pressure (5–50 mTorr) did not significantly affect the visible light transmittance of the GZO films. Figure 5(b) presents that the optical transmittance of the GZO films strongly depended on the film thickness. As the film thickness increased from 150 to 1500 nm, the average transmittance in the visible region (including the glass substrate) gradually decreased from 88.4% to 76.7%. The high visible transmittance of the prepared GZO films up to 88% is comparable to that of commonly used ITO films. Considering the results of the electrical properties, therefore, a suitable film thickness for TCO application should be in the range of 150–1000 nm.

In the UV region (below 380 nm), steep absorption edges were found (Figs. 5(a) and (b)). The shift of the absorption edge of the GZO film towards longer wavelengths (red-shift) with an increase in deposition pressure and film thickness. The absorption edge is usually related to the optical band gap ($E_{g,opt}$) for a degenerated semiconductor film. In 1968, Tauc proposed a method for estimating the optical band gap energy of amorphous semiconductors using optical absorption spectra [22]. In the method, the optical band gap energy is obtained by extrapolating the linear region in the graph of $(\alpha h\nu)^2$ versus $h\nu$ (photon energy) to the abscissa, where α is an absorption coefficient. The optical band gap energy was calculated by using the Tauc equation for semiconductor thin films [23].

$$\alpha h\nu = C(h\nu - Eg)^{\gamma} \quad (2)$$

where v is photon frequency and h is Planck constant. The exponent γ equals to 2 or 1/2 for the indirect or direct transition band gap, respectively [24]. The absorption coefficient α is calculated by adopting Beer-Lambert law [25].

$$\alpha = \frac{\ln\left(\frac{1}{T}\right)}{t} \tag{3}$$

where T and t are the transmittance and the film thickness, respectively. Figures 6(a) and 6(b) display plots of $(\alpha hv)^2$ as a function of incident photon energy (hv) for the GZO thin films with different deposition pressure and film thickness, respectively. All values of $E_{g,opt}$ were larger than that of undoped ZnO (~3.37 eV), indicating that the Ga dopant effectively widened the band gap of the film. The results showed that the $E_{g,opt}$ of the film decreased from 3.86 to 3.67 eV as the pressure increased from 5 to 20 mTorr, while slightly increased to 3.69 eV on further increasing the pressure to 50 mTorr. Marwoto et al. [11] also found that the optical band gap of GZO film was less variable at high Ar pressures. Besides, the $E_{g,opt}$ of the film increased from 3.79 to 3.86 eV as the film thickness increased from 70 to 330 nm, but a further increase in the thickness (from 330 to 1500 nm) resulted in gradually decreasing $E_{g,opt}$ to 3.75 eV. In general, the $E_{g,opt}$ of GZO thin films deposited by sputtering increase with an increase in carrier concentration. This relationship between $E_{g,opt}$ and carrier concentration was clarified by Burstein–Moss (BM) effect [26,27], which is expressed as follows [28].

$$\Delta E_g^{BM} = \frac{h^2}{8m_e^*}\left(\frac{3}{\pi}\right)^{\frac{2}{3}} n_e^{\frac{2}{3}} \tag{4}$$

where n_e and m_e* is electron concentration and electron effective mass, respectively. Free electrons fill up the states at the bottom of the conduction band when n_e exceeds the density of states at the edge of the conduction band and the Fermi level moves up within the conduction band. In this study, the BM effect has good applicability for the specimens prepared at different deposition pressures (5–20 mTorr) or film thicknesses (70–330 nm). However, for the specimens deposited with a thicker thickness (330–1500 nm) the band gap of the GZO film decreased with an increase in carrier concentration and film thickness. A similar phenomenon was also reported by Hao et al. [29] and Choi et al. [30] in AZO and IZTO thin films, respectively. This band gap reduction in degenerated semiconductors may be attributed to the merger of donors and conduction band, band tailing due to potential fluctuations caused by impurities, and electron-impurity and electron-electron scattering [31].

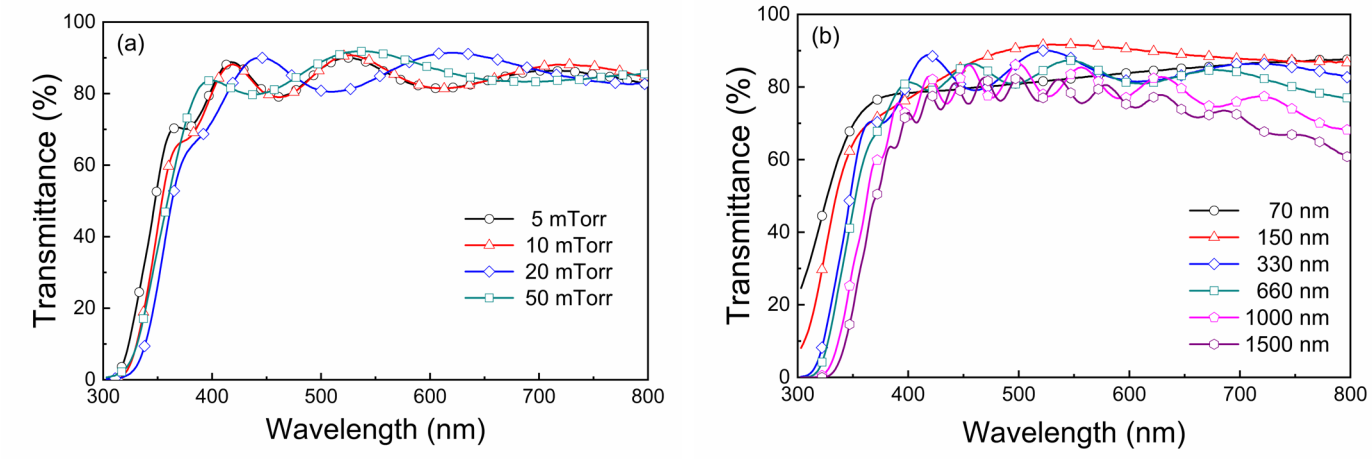

Fig. 5. Optical transmittance spectra of the GZO thin films with various thickness in the wavelength region of 400–700 nm.

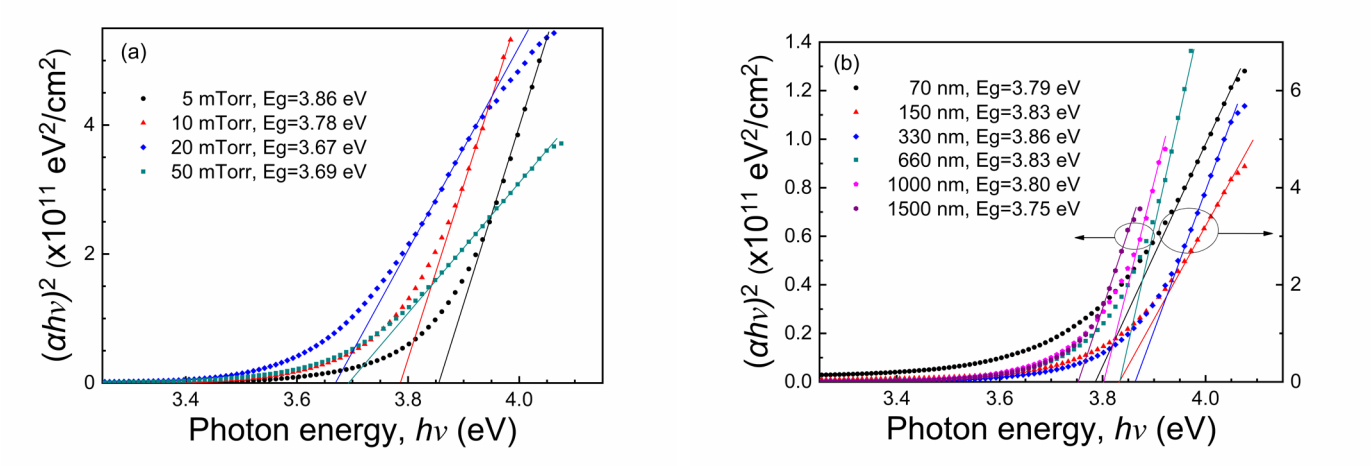

Fig. 6. Plots of $(\alpha hv)^2$ as a function of incident photon energy (hv) for the GZO thin films with different (a) deposition pressure and (b) film thickness.

To evaluate the optoelectrical property of transparent conductive thin films, Haacke's figure of merit (*FOM*) is adopted, which can be calculated by the following relation [32].

$$FOM = \frac{T^{10}}{R_S} \tag{5}$$

where T is average transmittance in the visible light region (400–700 nm) and R_S represents sheet resistance of the film. Figure 7 exhibits the figures of merits for the GZO thin films with various deposition pressures and film thicknesses. Figure 7(a) shows that as the deposition pressure increased from 5 to 50 mTorr, the *FOM* value gradually decreased. The sample with the pressure of 5 mTorr had the largest *FOM* value (1.17×10^{-2} Ω^{-1}). Figure 7(b) depicts that as the film thickness increased from 70 to 660 nm, the *FOM* value gradually increased and then leveled off with further increases in thickness to 1500 nm. The prepared GZO thin films achieved the highest *FOM* value of 3.09×10^{-2} Ω^{-1} at the thickness of 1000 nm and the pressure of 5 mTorr. This *FOM* value is higher than those of recently reported AZO and IZO thin films [33–36].

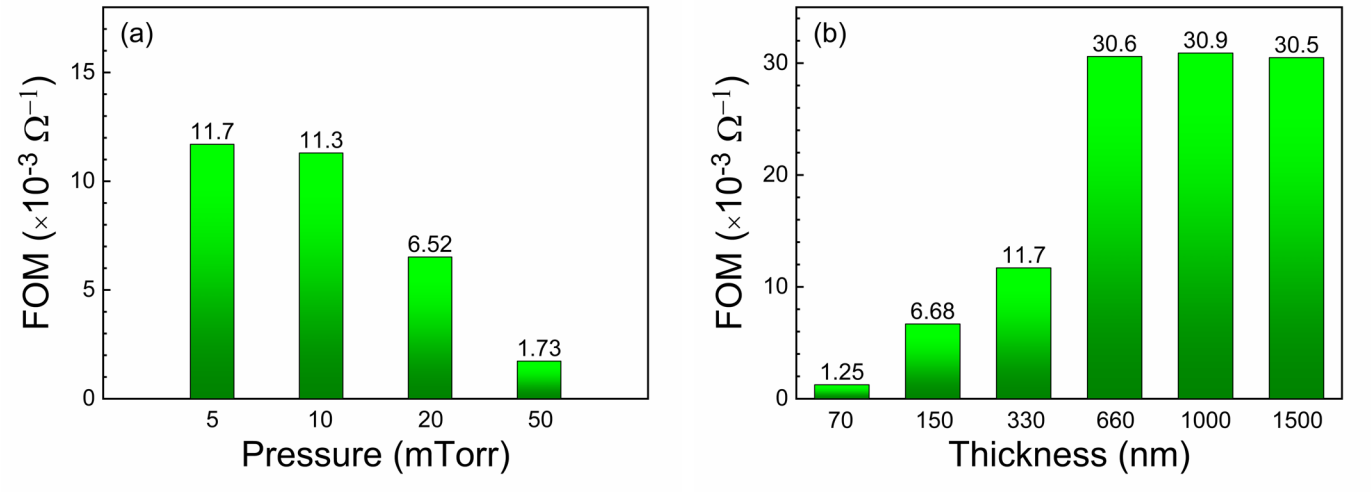

Fig. 7. Figures of merit of the GZO thin films as a function of (a) deposition pressure and (b) film thickness.

4. Conclusions

ZnO:Ga (3 wt%) thin films were prepared on glass substrates using RF magnetron sputtering. The dependence of the structural, electrical, and optical properties of the GZO films on deposition pressure (5–50 mTorr) and film thickness (70–1500 nm) was investigated. All the GZO thin films show a hexagonal wurtzite structure. Regardless of deposition pressure and film thickness the films were highly oriented to the c-axis perpendicular to the substrate surface. With decreasing deposition pressure and increasing film thickness, XRD results exhibited an improvement in crystal quality with a maximum grain size of 41 nm obtained at 5 mTorr and 330 nm. The electrical resistivity decreased with decreasing deposition pressure and increasing film thickness, and the lowest resistivity of 3.36×10^{-4} Ω-cm was achieved at 5 mTorr and 1000 nm. The average visible transmission remained at 84–86% regardless of deposition pressure, while it decreased from 88 to 76 % as the film thickness increased from 150 to 1500 nm. At the pressure of 5 mTorr and the thickness of 330 nm, the estimated optical band gap of the GZO thin film reached a maximum value of 3.86 eV. The FOM of the GZO thin films increased with decreasing pressure and increasing thickness, with the highest value of 3.09×10^{-2} Ω^{-1} obtained at 5 mTorr and 1000 nm. Such excellent optical and electrical properties, as well as high FOM, suggest that the fabricated GZO thin films are promising for applications of transparent conductive films and optoelectronic devices.

Author Contributions: Conceptualization, F.H. Wang; methodology, F.H. Wang and H.T. Tzeng; validation, F.H. Wang and H.T. Tzeng; formal analysis, F.H. Wang and H.T. Tzeng; investigation, F.H. Wang and H.T. Tzeng; data curation, F.H. Wang and H.T. Tzeng; writing—original draft preparation, F.H. Wang; writing—review and editing, F.H. Wang. All authors have read and agreed to the published version of the manuscript.

Acknowledgments: This work was supported by projects under Nos. MOST 107-2221-E-005-048 and MOST 109-2221-E-005-076.

Conflicts of Interest: The authors declare no conflict of interest.

References

1. Minami, T.; Nanto, H.; Takata, S. Highly conductive and transparent aluminum doped zinc oxide thin films prepared by rf magnetron sputtering. *Jpn. J. Appl. Phys.* **1984**, *23*, L280–L282. https://doi.org/10.1143/JJAP.23.L280
2. Hoshi, Y.; Kiyomura, T. ITO thin films deposited at low temperatures using a kinetic energy controlled sputter-deposition technique. *Thin Solid Films* **2002**, *411*, 36–41. https://doi.org/10.1016/S0040-6090(02)00170-0
3. Li, C.; Furuta, M.; Matsuda, T.; Hiramatsu, T.; Furuta, H.; Hirao, T. Characterisation of sol–gel silica films doped with chromium (III) acetylacetonate. *Thin Solid Films* **2009**, *517*, 3265–3628. https://doi.org/10.1016/j.tsf.2008.11.109
4. Lin, Y.C.; Jiang, J.H.; Yen, W.T. Effect of Cr and V dopants on the chemical stability of AZO thin film. *Appl. Surf. Sci.* **2009**, *255*, 3629–3634. https://doi.org/10.1016/j.apsusc.2008.10.019
5. Wang, F.H.; Chang, H.P.; Tseng, C.C.; Huang, C.C. Effects of H_2 Plasma Ttreatment on Properties of ZnO:Al Thin Films Prepared by RF Magnetron Sputtering. *Surf. Coat. Technol*. **2011**, *205*, 5269–5277. https://doi.org/10.1016/j.surfcoat.2011.05.033
6. Minami, T.; Sato, H.; Nanto, H.; Takata, S. Group III impurity doped zinc oxide thin films prepared by rf magnetron sputtering. *Jpn. J. Appl. Phys*. **1985**, *24*, L781–L784. https://doi.org/10.1143/JJAP.24.L781
7. Flickyngerová, S.; Netrvalová, M.; Šutta, P.; Novotný, I.; Tvarožek, V.; Gašpierik, P.; Bruncko, J. Effects of sputtering power and pressure on properties of ZnO:Ga thin films prepared by oblique-angle deposition. *Thin Solid Films* **2011**, *520*, 1233–1237. https://doi.org/10.1016/j.tsf.2011.06.073
8. Yu, C.F.; Chena, S.H.; Sun, S.J.; Chou, H. Influence of the grain boundary barrier height on the electrical properties of Gallium doped ZnO thin films. *Appl. Surf. Sci*. **2011**, *257*, 6498–6502. https://doi.org/10.1016/j.apsusc.2011.02.051
9. Wang, F.H.; Fu, M.Y.; Su, C.C.; Yang, C.F; Tzeng, H.T.; Liu, H.W.; Kung, C.Y. Improve the Properties of p-i-n α-Si:H Thin-Film Solar Cells Using the Diluted Hydrochloric Acid-Etched GZO Thin Films. *J. Nanomater.* **2013**, 495752. http://dx.doi.org/10.1155/2013/495752
10. Wu, J.L.; Chen, Y.C.; Lin, H.Y.; Chu, S.Y.; Chang, C.C.; Wu, C.J.; Juang, Y.D. Effect of ZnO Buffer Layer on the Bending Durability of ZnO:Ga Films Grown on Flexible Substrates: Investigation of Surface Energy, Electrical, Optical, and Structural Properties. *IEEE T. Electron Dev.* **2013**, *60*, 2324–2329. http://doi.org/10.1109/TED.2013.2259491
11. Marwoto, P.; Fatiatun; Sulhadi; Sugianto; Aryanto, D. Effects of argon pressure on the properties of ZnO:Ga thin films deposited by DC magnetron sputtering. AIP Conference Proceedings **2016**, *1719*, 030016. http://doi.org/10.1063/1.4943711
12. Kim, D.K.; Kim, H.B. Initial vacuum effects on the properties of sputter deposited Ga-doped ZnO thin films. *J. Alloys Compd.* **2017**, *709*, 627–632. https://doi.org/10.1016/j.jallcom.2017.03.189
13. Peng, L.P.; Fang, L.; Yang, X.F.; Ruan, H.B.; Li, Y.J.; Huang, Q.L.; Kong, C.Y. Characteristics of ZnO:In thin films prepared by RF magnetron sputtering, *Phys. E* **2009**, *41*, 1819–1823. https://doi.org/10.1016/j.physe.2009.07.006

14. Zhou, H.B.; Zhang, H.Y.; Tan, M.L.; Zhang, W.J.; Zhang, W.L. Effects of sputtering pressure on properties of Al doped ZnO thin films dynamically deposited by rf magnetron sputtering. *Mater. Res. Innovations* **2012**, *16*, 390–394. https://doi.org/10.1179/1433075X12Y.0000000002
15. Das, R.; Jana, T.; Ray, S. Degradation studies of transparent conducting oxide: a substrate for microcrystalline silicon thin film solar cells. *Sol. Energy Mater. Sol. Cells* **2005**, *86*, 207–216. https://doi.org/10.1016/j.solmat.2004.07.009
16. Fang, L.; Wu, F.; Huang, Q.L.; Yang, X.F.; Kong, C.Y. Effect of Ga Doping Concentration on Electrical and Optical Properties of Nano-ZnO:Ga Transparent Conductive Films, *J. Supercond. Nov. Magn*. **2010**, *23*, 885–888. https://doi.org/10.1007/s10948-010-0705-0
17. Meng, L.J.; Dos Santos, M.P. Direct current reactive magnetron sputtered zinc oxide thin films, *Thin Solid Films* **1994**, *250*, 26–32. https://doi.org/10.1016/0040-6090(94)90159-7
18. Sanon, G.; Rup, R.; Mansingh, A. Growth and characterization of tin oxide films prepared by chemical vapour deposition. *Thin Solid Films* **1990**, *190*, 287–301. https://doi.org/10.1016/0040-6090(89)90918-8
19. Wu, F.;·Fang, L.; ·Zhou, K.; ·Pan, Y.J.;·Peng, L.P.; Huang, Q.L.; ·Yang, X.F.; ·Kong, C.Y. Effect of Thickness on the Properties of Ga-doped Nano-ZnO Thin Films Prepared by RF Magnetron Sputtering. *J. Supercond. Nov. Magn.* **2010**, *23*, 905–908. https://doi.org/10.1007/s10948-009-0637-8
20. Shin, S.W.; Pawa, S.M.; Kim, T.W.; Moon, J.H.; Kim, J.H. Effect of film thickness on the structural and electrical properties of Ga-doped ZnO thin films prepared on glass and Al_2O_3 (0001) substrates by RF magnetron sputtering method. · *J. Mater. Res.* **2009**, *24*, 441–447. https://www.researchgate.net/publication/259104348
21. Chang, H.P; Wang, F.H,; Chao, J.C.; Huang, C.C.; Liu, H.W. Effects of thickness and annealing on the properties of Ti-doped ZnO films by radio frequency magnetron sputtering. *Curr. Appl. Phys.* **2011**, *11*, S185–S190. http://doi:10.1016/j.cap.2010.11.110
22. Tauc, J. Optical properties and electronic structure of amorphous Ge and Si. *Mater. Res. Bull*. **1968**, *3*, 37–46. http://doi:10.1016/0025-5408(68)90023-8
23. Tauc, J. Absorption edge and internal electric fields in amorphous semiconductors. *Mater. Res. Bull.* **1970**, *5*, 721–729. https://doi.org/10.1016/0025-5408(70)90112-1
24. Coulter, J.B.; Birnie III, D.P. Assessing Tauc plot slope quantification: ZnO thin films as a model system. *Phys. Status Solidi B* **2018**, *255*, 1700393. https://doi.org/10.1002/pssb.201700393
25. Shanmuganathan, G.; Shameem Banu, I.B.; Krishnan, S.; Ranganathan, B. Influence of K-doping on the optical properties of ZnO thin films grown by chemical bath deposition method. *J. Alloys Compd*. **2013**, *562*, 187–193. https://doi.org/10.1016/j.jallcom.2013.01.184
26. Burstein, E. Anomalous optical absorption limit in InSb. *Phys. Rev.* **1954**, *93*, 632–633. https://doi.org/10.1103/PhysRev.93.632
27. Moss, T.S. The interpretation of the properties of indium antimonide. *Proc. Phys. Soc. Sect. B* **1954**, *67*, 775–782. https://doi.org/10.1088/0370-1301/67/10/306
28. Sernelius, B.E.; Berggren, K.F.; Jin, Z.C.; Hamberg, I.; Granqvist, C.G. Band-gap tailoring of ZnO by means of heavy Al doping. *Phys. Rev. B* **1988**, *37*, 10244–10248. https://doi.org/10.1103/PhysRevB.37.10244
29. Hao, X.; Ma, J.; Zhang, D.; Yang, T.; Ma, H.; Yang, Y.; Cheng, C.; Huang, J. Thickness dependence of structural, optical and electrical properties of ZnO:Al films prepared on flexible substrates. *Appl. Surf. Sci.* **2001**, *183*, 137–142. https://doi.org/10.1016/S0169-4332(01)00582-7
30. Choi, K.-H.; Jeong, J.-A; Kim, H.-K. Dependence of electrical, optical, and structural properties on the thickness of IZTO thin films grown by linear facing target sputtering for organic solar cells. *Sol. Energy Mater. Sol. Cells* **2010**, *94*, 1822–1830. https://doi.org/10.1016/j.solmat.2010.05.056
31. Han, H.; Mayer, J.W.; Alford, T.L. Band gap shift in the indium–tin–oxide films on polyethylene napthalate after thermal annealing in air. *J. Appl. Phys*. **2006**, *100*, 083715-1–083715-6. https://doi.org/10.1063/1.2357647
32. Haacke, G. New figure of merit for transparent conductors. *J. Appl. Phys*. **1976**, *47*, 4086. https://doi.org/10.1063/1.323240
33. Sarma, B.; Barman, D.; Sarma, B.K. AZO (Al:ZnO) thin films with high figure of merit as stable indium free transparent conducting oxide. *Appl. Surf. Sci.* **2019**, *479*, 786–795. http://doi.org/10.1016/j.apsusc.2019.02.146
34. Tsai, D.C.; Chang, Z.C.; Kuo, B.H.; Wang, Y.H.; Chen, E.C.; Shieu, F.S. Thickness dependence of the structural, electrical, and optical properties of amorphous indium zinc oxide thin films. *J. Alloys Compd.* **2018**, *743*, 603–609. https://doi.org/10.1016/j.jallcom.2017.12.062
35. Kumar, N, Chowdhury, A.H.; Bahrami, B.; Khan, M.R.; Qiao, Q.; Kumar, M. Origin of enhanced carrier mobility and electrical conductivity in seed-layer assisted sputtered grown Al doped ZnO thin films. *Thin Solid Films* **2020**, *700*, 137916. https://doi.org/10.1016/j.tsf.2020.137916
36. Challali, F.; Mendilm, D.; Touam, T.; Chauveau, T.; Sanchez, A.G.; Chelouche, A.; Besland, M.-P. Effect of RF sputtering power and vacuum annealing on the properties of AZO thin films prepared from ceramic target in confocal configuration. *Mater. Sci. Semicond. Process*. **2020**, *118*, 105217. https://doi.org/10.1016/j.mssp.2020.105217